 ©2010 Kvantovaya Elektronika and Turpion Ltd

PACS numbers: 87.64.km; 87.85.Rs; 78.67.Bf
DOI: 10.1070/QE2010v040n12ABEH014472

Spectroscopy of nanoparticles based on $Gd_{14}B_6Ge_2O_{34}$ polycrystals and $La_2O_3-B_2O_3$ glasses, activated by Nd^{3+} ions, for cancer diagnostics

A.V. Popov, A.V. Ryabova, M.G. Komova, V.A. Krut'ko, O.B. Petrova, V.B. Loshchenov, Yu.K. Voron'ko

Abstract. **Nanoparticles of gadolinium borate polycrystals and borate glasses, activated by Nd^{3+} ions, are obtained from bulk samples of the corresponding compositions by mechanical grinding and ultrasonic dispersion in water. A spectroscopic study of these nanoparticles in the near-IR region is performed to determine their potential as luminescence biosensors and radiopharmaceutical preparations for cancer diagnostics by radiosensitive methods. A twofold increase in the lifetime of the metastable $^4F_{3/2}$ state of Nd^{3+} ions at the transition from submicron polycrystalline particles to nanoparticles is experimentally found. A study of the nanoparticle distribution over organs and tissues of laboratory animals, performed with a 810-nm laser for exciting luminescence and a multichannel fibre spectrometer for measuring fluorescence in the range of 0.8–1.2 μm, showed this technique to be sufficiently sensitive to reliably determine the nanoparticle concentration in biological tissues and the dynamics of its change.**

Keywords: *in vivo fluorescence spectroscopy, nanoparticles of polycrystals and glasses, rare earth ions.*

1. Introduction

The methods of cancer diagnostics based on the use of radiopharmaceutical preparations make it possible to perform diagnostics of rather large tumours of inner organs, including metastases 5–7 mm in size [1], whereas fluorescent analysis has significant advantages in the case at planar epithelial cancer forms and allows one to detect very small (to 1 mm) tumours in surface layers. Fluorescent diagnostics can be implemented with the aid of fluorescence video cameras, fluorescence attachments for endoscopic systems and operational microscopes, and fibre spectrometers when lasers are used to excite fluorescence in endogenous and/or exogenous fluorophors. In principle these approaches can be combined when applying nanoparticles of gadolinium (Gd^{3+}) borate crystals and glasses activated by rare earth (RE) ions.

A.V. Popov, A.V. Ryabova, V.B. Loshchenov, Yu.K. Voron'ko
A.M. Prokhorov General Physics Institute, Russian Academy of Sciences, ul. Vavilova 38, 119991 Moscow, Russia;
e-mail: avpopov@lst.gpi.ru, nastya.ryabova@gmail.com, loschenov@mail.ru, voronko@lst.gpi.ru;
M.G. Komova, V.A. Krut'ko N.S. Kurnakov Institute of General and Inorganic Chemistry, Russian Academy of Sciences, Leninsky prosp. 31, 119991 Moscow, Russia; e-mail: Kroutko@igic.ras.ru;
O.B. Petrova D.I. Mendeleev Russian University of Chemical Technology, Miusskaya pl. 9, 125047 Moscow, Russia; e-mail: petrova@proriv.ru

Received 30 September 2010; revision received 28 October 2010
Kvantovaya Elektronika **40** (12) 1094–1097 (2010)
Translated by Yu.P. Sin'kov

Rare earth ions Nd^{3+}, Tm^{3+}, and Yb^{3+} exhibit absorption and luminescence electronic transitions in the near-IR range from 0.75 to 1.1 μm, which coincides with the transparency window of biological tissues. This circumstance makes it possible to excite and record luminescence of RE ions in nanoparticles located in biological tissues in the spectral range where the intrinsic autofluorescence is low, and the penetration depth of laser radiation reaches 8–10 mm. The presence of narrow strong luminescence lines of RE ions also significantly increases the signal-to-noise ratio when detecting the luminescence signal. Here, the 'noise' is considered to be, in particular, the intrinsic fluorescence of biological tissue chromophores.

The compounds containing Gd^{3+} ions are widely used in clinical practice for cancer diagnostics. In magnetic resonance tomography (MRT), which is based on NMR spectroscopy, low-molecular (Gd–DTPA, etc.) and high-molecular [albumin–$(Gd–DTPA)_n$, dextrane–$(Gd–DTPA)_n$] Gd-based metalloporphyrins, introduced into the vascular network, are used as a contrasting material to visualise biological tissues with a high resolution [2]. In this context, it is expedient to use nanoparticles of Gd-based inorganic compounds for MRT diagnostics.

In this paper we report the results of the initial stage of the study aimed at developing nanomaterials based on inorganic complex-anion gadolinium compounds activated by near-IR luminescent RE ions for multifunctional cancer diagnostics. We investigated the spectroscopic properties of submicron and nanosized particles (from several nanometers to several hundreds of nanometers) of $Gd_{14}(BO_3)_6(GeO_4)_2O_8$ borate polycrystals and $La_2O_3-B_2O_3$ glasses, activated by RE ions, in the solid state, in aqueous solutions, and in organs and tissues of experimental animals. The problems related to the analysis and interpretation of spectroscopic properties of RE ions in a dielectric medium upon transition from macro- to nanoparticles have been actively discussed in the literature [3–9]. According to the results of these studies, the lifetimes of the metastable states of RE ions in nanoparticles may increase (under certain conditions) by a factor of 2 or more in comparison with bulk crystals [6, 7]. This effect was theoretically justified in [9], where a formula characterising the increase in the lifetime of the states with a decrease in the nanoparticle size was reported; nevertheless, the experimental verification, showing the applicability limits for this dependence, is insufficient.

2. Objects of study and experiment

Polycrystals of gadolinium borate germanates $Gd_{14}(BO_3)_6(GeO_4)_2O_8$:$Nd^{3+}$ with Nd^{3+} concentrations of 0.5, 3.0, and 7.0 at % with respect to Gd^{3+} (Table 1) were obtained by

Table 1. Lifetimes of the $^4F_{3/2}$ level of Nd^{3+} ions in aqueous ($n = 1.33$) colloidal solutions of nanoparticles and micrometer-sized (0.5–1.0 μm) particles

Composition	Nanoparticle size/nm	Excitation wavelength/nm	Measurement wavelength/nm	Lifitime in nanoparticles/μs	Lifetime in micrometer-sized nanoparticles/μs
$Gd_{14}(BO_3)_6(GeO_4)_2O_8$: 0.5 at% Nd^{3+}	78–200	803	880	80	80
$Gd_{14}(BO_3)_6(GeO_4)_2O_8$: 3.0 at% Nd^{3+}	42–500	803	880	50	50
$Gd_{14}(BO_3)_6(GeO_4)_2O_8$: 7.0 at% Nd^{3+}	5, 32–500	803	880	70	33

solid-phase synthesis at $T = 1520$ K [10]. Lanthanum borate glass $La_2O_3-B_2O_3$, containing 1 mol % Nd_2O_3, was synthesised in a corundum crucible in air and poured onto a cooled brass substrate. Aqueous colloidal solutions of nanoparticles were obtained from bulk samples of the corresponding compositions in several stages by mechanical grinding and ultrasonic dispersion in water. The hydrodynamic radii of submicron and nanosized particles were measured using a dynamic Photocor Complex light scattering spectrometer. A mathematical analysis of the correlation function showed that the aqueous colloidal solutions contained, along with nanoparticles of different sizes, submicron particles with hydrodynamic radii up to 500 nm. The characteristic hydrodynamic radii of the nanoparticles corresponding to the strongest lines in the dynamic light scattering spectra of aqueous solutions of these particles are listed in Table 1. The error in measuring the hydrodynamic radii of the particles is ±1%.

The diameters of pores in the blood vessels feeding a cancer tumour are known to be 10–500 nm; i.e., they greatly exceed the sizes of pores in the blood vessels of healthy organs (2–6 nm). Therefore, address delivery of particles from blood circulation through pores in blood vessels to a cancer tumour calls for nanoparticles with sizes above 10 nm. Otherwise nanoparticles do not have a good selectivity of accumulation in malignant tumours in comparison with a normal tissue without an additional coating; however, they can be used for fluorescent visualisation and therapy, when conjugated with peculiar anticarcinogenic antibodies.

We performed a spectral analysis of the luminescence of Nd^{3+} ions on a double SDL-1 monochromator (LOMO). Samples of two types were studied: aqueous colloidal solutions of nanoparticles and submicron particles placed in a quartz cell (samples of type 1) or between cover glasses (type 2). The thickness of the water layer in samples 2 was 10 ± 1 μm. The luminescence spectra of the samples of both types were recorded in a longitudinal (with respect to the excitation laser beam) geometry. The luminescence decay kinetics of Nd^{3+} ions was investigated upon excitation by a 10-ns pulsed Al_2O_3 : Ti laser. In samples of type 1 the luminescence decay was recorded in the direction perpendicular to the excitation laser beam.

Fluorescence studies on laboratory animals were performed using a laser electronic LESA-01-Biospec spectrum analyser [11], which was modified by attaching an additional 810-nm cw IR laser and the corresponding optical filters.

The system for backward scattering measurements (Fig. 1) includes a spectrometer; a light source with focusing optics (halogen lamp and laser for absorption and fluorescence measurements, respectively); a portable computer; a software for processing spectra (UnoMomento-Biospec); and a flexible optical catheter, which consists of an optical fibre at the centre for transmitting laser radiation and six fibres around for receiving scattered laser radiation and the fluorescence signal. A schematic of measurements at the point of contact between the optical catheter and a biological object is shown in Fig. 2. Laser radiation is multiply scattered in the sample and induces

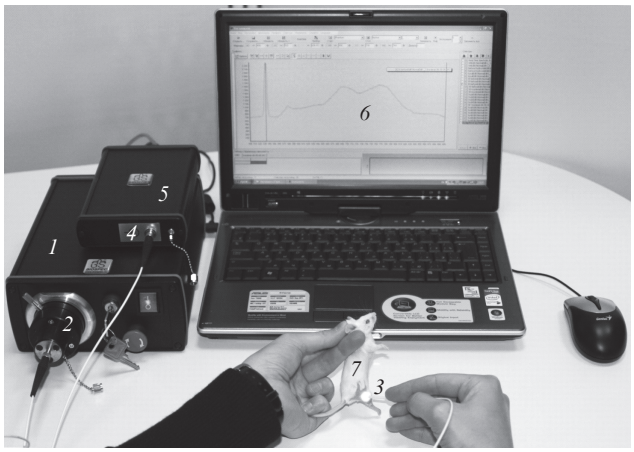

Figure 1. LESA-01-Biospec fiber system for *in vivo* spectral measurements on experimental animals:
(*1*) laser; (*2*) fibre adapter; (*3*) fibre catheter; (*4*) spectral filter; (*5*) spectrometer; (*6*) software; (*7*) biological sample.

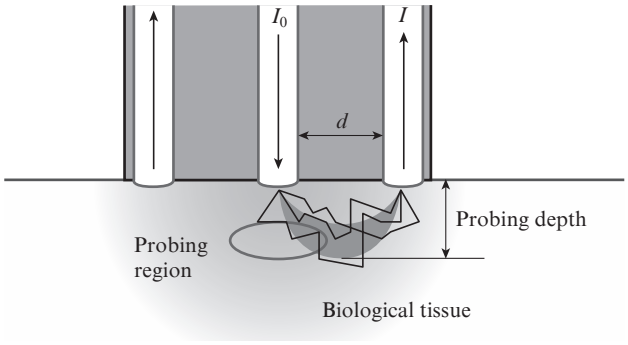

Figure 2. Light propagation in a sample under study in the region of contact with the distal end of the flexible optical catheter.

fluorescence before arriving at the receiving optical fibres. It is the volume of the biological sample between the feed and receiving fibres that contributes to the fluorescence signal. The sample probe depth can be varied by changing the distance d between the fibres. In this study d was chosen to be 250 μm, and the probe depth did not exceed 3 mm.

The spectral characteristics of the nanoparticles studied demonstrated a high (equal to 8) signal-to-noise ratio at their concentration of 5 mg kg^{-1} in the biological tissue.

3. Discussion of the main results

The experimental lifetime of Nd^{3+} ions at the $^4F_{3/2}$ level in $Gd_{14}(BO_3)_6(GeO_4)_2O_8$: 7 at % Nd^{3+} nanoparticles exceeds that in submicron particles by a factor of 2 (Table 1). This result follows from Fig. 3, which shows the decay kinetics of this level for $Gd_{14}(BO_3)_6(GeO_4)_2O_8$ nanoparticles with different contents of Nd^{3+} ions. Luminescence decay curves (*1*) and (*3*) have similar slopes in the $\ln I - t$ coordinates, which is

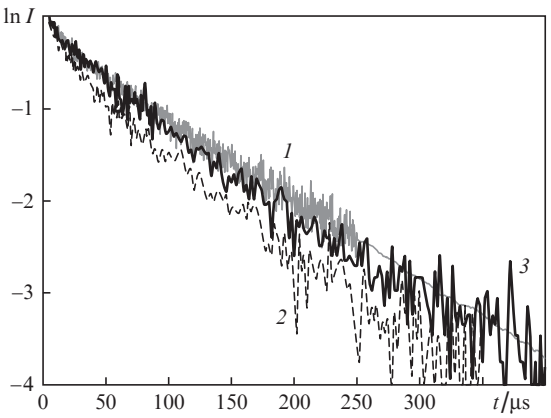

Figure 3. Luminescence decay kinetics of the $^4F_{3/2}$ level of Nd^{3+} ions in nanoparticles of $Gd_{14}(BO_3)_6(GeO_4)_2O_8$ polycrystals with Nd^{3+} concentrations of (*1*) 0.5, (*2*) 3, and (*3*) 7 at %.

indicative of similar lifetimes of the $^4F_{3/2}$ level in these nanoparticles with neodymium concentrations of 0.5 and 7 at%, although the decay of the $^4F_{3/2}$ level should significantly increase with an increase in the Nd^{3+} concentration. The decay enhancement is due to the nonradiative energy transfer between Nd^{3+} ions as a result of cross-relaxation ($^4F_{3/2}$–$^4I_{15/2}$, $^4I_{9/2}$–$^4I_{15/2}$) (Table 1).

This important result qualitatively confirms formula (1), which was obtained in [9] for spherical nanoparticles. Most necessary conditions for this formula were implemented in our experiments. For example, the refractive index of polycrystalline particles ($n_{cr} \sim 2$) significantly exceeds that of water ($n_{med} = 1.33$), and the volume concentration of nanoparticles in a colloidal solution is close to zero ($c \to 0$). The ratio of the lifetimes of the activator metastable level in nanoparticles and in a bulk crystal is

$$\frac{\tau_{nano}}{\tau_{bulk}} = \frac{n_{cr}}{n_{med}}\left[\frac{2+\varepsilon}{3}\right]^2, \qquad (1)$$

where n_{cr} and n_{med} are, respectively, the refractive indices of nanoparticles (or a bulk crystal) and the medium around them and $\varepsilon = n_{cr}^2/n_{med}^2$ is the ratio of their dielectric constants.

The lifetimes of the $^4F_{3/2}$ level of Nd^{3+} ions in $Gd_{14}(BO_3)_6(GeO_4)_2O_8$ with Nd^{3+} concentrations of 0.5 and 3 at % is independent of the particle size (Table 1). This can be explained by the larger particle sizes (78 and 42 nm, respectively, for Nd^{3+} concentrations of 0.5 and 3 at %) in comparison with $Gd_{14}(BO_3)_6(GeO_4)_2O_8$: 7 at % Nd^{3+} nanoparticles, whose minimum sizes were 5 and 32 nm. A significant deviation from the theoretical dependence (1) was observed for La_2O_3–B_2O_3 : 1.0 wt % Nd_2O_3 glass particles (Table 1).

The increase in the luminescence lifetime τ_{nano} with a simultaneous increase in the luminescence intensity from RE ions in nanoparticles, which are used as biolabels, is of practical interest. This increase makes it possible to easily record *in vivo* the luminescence signal of such biolabels (in the spectral range overlapping the range of much stronger but shorter autoluminescence of biological tissues) by detecting the luminescence spectra of RE ions with a time delay of 10–20 μs and a time window of 100 μs or more. As a result, the technical requirements to the spectral-diagnostic equipment for measuring luminescence spectra with this time resolution become less strict.

The shape of the luminescence spectra of Nd^{3+} ions only slightly depends on the particle size (Fig. 4). We established this fact when recording the luminescence spectra of the samples of two types (see Section 2), composed of $Gd_{14}(BO_3)_6(GeO_4)_2O_8$: 7 at % Nd^{3+} polycrystalline particles of different sizes [Fig. 4, spectra (*2*–*4*)]. The luminescence spectra of Nd^{3+} ions in glass nanoparticles [Fig. 4, spectrum (*1*)] and in bulk glasses [12] are similar.

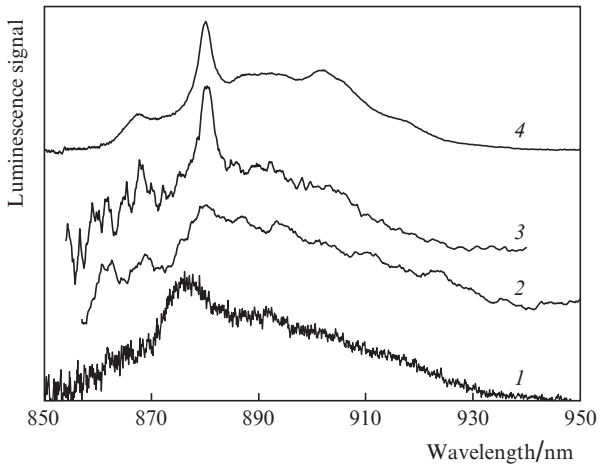

Figure 4. Luminescence spectra of Nd^{3+} ions at the $^4F_{3/2}$–$^4I_{9/2}$ transition in (*1*) nanoparticles of La_2O_3–B_2O_3 : 1.0 wt % Nd_2O_3 glasses (sample 1), (*2*) nanoparticles of $Gd_{14}(BO_3)_6(GeO_4)_2O_8$: 7 at % Nd^{3+} polycrystals (sample 2), (*3*) nanoparticles of $Gd_{14}(BO_3)_6(GeO_4)_2O_8$: 7 at % Nd^{3+} polycrystals (sample 1), and (*4*) submicron $Gd_{14}(BO_3)_6(GeO_4)_2O_8$: 7 at % Nd^{3+} particles (sample 2).

We performed a preliminary study of the pharmacokinetics of nanoparticles (5 and 32 nm in size) and submicron particles (to 500 nm) of $Gd_{14}(BO_3)_6(GeO_4)_2O_8$: 7 at % Nd^{3+} polycrystals on laboratory mice with Ehrlich carcinomas interwoven into the muscular tissue of hindlegs. An aqueous colloidal solution of nanoparticles (volume 0.2 mL, concentration 2 mg mL^{-1}) was introduced intravenously. The preparation dose per animal mass was 16 mg kg^{-1}.

The distribution of these nanoparticles over the mouse organs and tissues 1 h after the administration was found using fluorescence spectroscopy (Table 2). To quantitatively determine the nanoparticle concentration from the luminescence spectra, we measured the spectra of scattering phantoms (which are similar to biological tissues in the optical range under study), containing different dilutions of nanoparticles. After plotting the dependence of the luminescence intensity on the number of nanoparticles in a phantom, we could determine the nanoparticle concentration in biological tissues from the luminescence intensity with an error to 10%.

Table 2. Concentrations of nanoparticles and submicron particles of polycrystalline $Gd_{14}(BO_3)_6(GeO_4)_2O_8$: 7.0 at % Nd^{3+} in the organs of a laboratory mouse after intravenous introduction (dose 16.0 mg kg^{-1}).

Inner organ	Concentration/mg kg^{-1}
Liver	20.0
Spleen	10.3
Kidney	5.6
Lungs	71.1

The particle distribution over inner organs was determined using an LESA-1 spectrometer on both living and prepared mice 1 h after the preparation administration. The luminescence spectra of Nd^{3+} ions (Fig. 5) were recorded from nanoparticles in the inner organs of the living mouse. After its preparation the luminescence spectra from each inner organ under study were measured again. The relative ratios of the maxima of luminescence lines of Nd^{3+} ions in these two recording versions of luminescence spectra hardly differ.

It can be seen in Fig. 5 that preparation particles are accumulated mainly in the lungs and liver of the laboratory mouse. The nanoparticle distribution over organs depends strongly on several factors: their size, surface charge, and the type of polymer coating. To develop this field of research, it appears to be important to analyse the effect of these factors on the nanoparticle distribution over tissues and organs of a normal organism and in organisms having some pathologies, in particular, malignant tumours and atherosclerotic changes in vessels. We did not observe any pronounced toxic effect after the intravenous administration of preparation; no intoxication symptoms were observed during the next two weeks either.

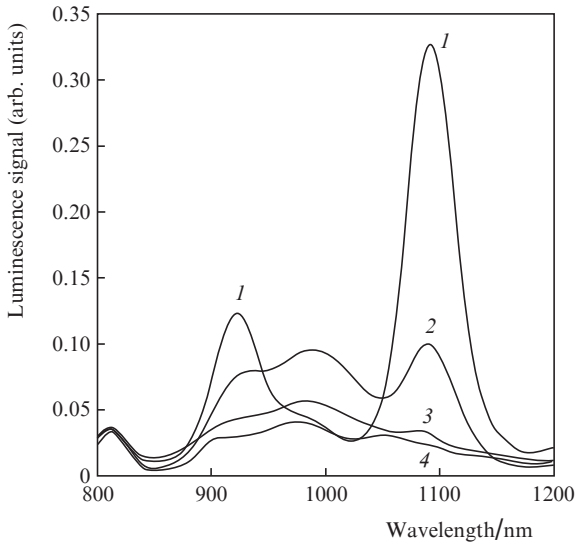

Figure 5. Luminescence spectra of Nd^{3+} ions at the $^4F_{3/2}-{}^4I_{9/2}$ and $^4F_{3/2}-{}^4I_{11/2}$ transitions in particles of $Gd_{14}(BO_3)_6(GeO_4)_2O_8$: 7 at% Nd^{3+} polycrystals, accumulated in (*1*) lungs, (*2*) liver, (*3*) spleen, and (*4*) kidney 1 h after intravenous administration.

4. Conclusions

We obtained colloidal solutions of nanoparticles and submicron particles of $Gd_{14}(BO_3)_6(GeO_4)_2O_8$ gadolinium borate-germanate polycrystals and borate glasses, activated by luminescent Nd^{3+} ions, and performed a preliminary study of the pharmacokinetics of these particles on laboratory mice with interwoven Ehrlich carcinomas. The spectroscopic characteristics of the particle solutions obtained were experimentally determined. In particular, it was found that the shape of the luminescence spectra of Nd^{3+} ions barely depends on the particle size, while the lifetime of the $^4F_{3/2}$ excited state of Nd^{3+} ions significantly increases when passing from bulk polycrystalline particles to nanoparticles.

Acknowledgements. This study was supported by Grant MK-105.2010.2 of the President of the Russian Federation for Support of Young Scientists.

References

1. http://netoncolofy.ru/expert/diagnostics/diagnostic_methods/1398/.
2. Sviridov N.K., Kotlyarov P.M. *Med. Vizual.*, **3**, 54 (1998).
3. Li Q., Gao L., Yan D. *Nanostr. Mater.*, **8**, 825 (1997).
4. Sun L., Liao C., Yan C. *J. Sol. State Chem.*, **171**, 304 (2003).
5. Song H., Chen B., Sun B., Zhang J., Lu S. *Chem. Phys. Lett.*, **372**, 368 (2003).
6. Boyer J.C., Vetrone F., Capobianco J.A., Speghini F., Bettinelli M. *J. Phys. Chem. B*, **108**, 20137 (2004).
7. Meltzer R.S., Feofilov S.P., Tissue B., Yuan H.B. *Phys. Rev. B*, **60**, R14012 (1999).
8. Dolgaleva K., Boyd R.W., Milonni P.W. *J. Opt. Soc. Am. B*, **24**, 516 (2007).
9. Basiev T.T., Orlovskii Yu.V., Pukhov K.K. *Ross. Nanotekhnol.*, **3**, 66 (2008).
10. Krut'ko V.A., Lysanova G.V., Burkov V.I., Bandurkin G.A., Komova M.G. *Neorg. Mater.*, **38**, 1364 (2002).
11. Loschenov V.B., Konov V.I., Prokhorov A.M. *Laser Phys.*, **10**, 1188 (2000).
12. Voron'ko Yu.K., Galaktionov S.S., Dmitruk L.N., Petrova O.B., Popov A.V., Ushakov S.N., Shukshin V.E. *Fiz. Khim. Stekla*, **32**, 69 (2006).